Chemical and Process Engineering: New Frontiers, 2025, 46(3), e105
DOI: 10.24425/cpe.2025.155543

Fabrication and microstructural studies of porous non-isocyanate polyurethanes (NIPU) and NIPU/POSS hybrid nanomaterials obtained with the particle leaching method

Piotr Stachak[1,*], Paulina Korzeniak[1], Edyta Hebda[1], Sebastian Wroński[2], Jacek Tarasiuk[2], Jan Ozimek[1,*], Krzysztof Pielichowski[1]

[1] Cracow University of Technology, Faculty of Chemical Engineering and Technology, Department of Chemistry and Technology of Polymers, Warszawska 24, 31-155 Kraków, Poland
[2] AGH University of Krakow, Faculty of Physics and Applied Computer Science, Department of Condensed Matter Physics, al. Mickiewicza 30, 30-059 Kraków, Poland

*** Corresponding author, e-mail:**
stachak.pe@gmail.com,
jan.ozimek@pk.edu.pl

Article info:
Received: 30 April 2025
Revised: 31 July 2025
Accepted: 25 August 2025

Abstract
Non-isocyanate polyurethanes (NIPUs) were synthesised by reacting trifunctional cyclic carbonate with poly(propylene oxide)-derived diamine and further chemically modified with polyhedral oligomeric silsesquioxane (POSS) moieties to obtain NIPU/POSS hybrids. The materials were manufactured in a porous form using sodium bicarbonate in the particle leaching method. FTIR spectra confirmed the creation of urethane groups in the synthesised materials and the incorporation of POSS particles into the NIPU matrix in the reaction between the oxirane rings present in POSS and the used amines. The SEM and computer micro-tomography (μ-CT) images obtained confirmed that the use of the selected size of the sodium bicarbonate crystals allowed pores to be obtained with controlled dimensions. The amount of POSS added (5, 10 and 15 wt.%) did not affect the pore size or its shape. Initial submersion studies using Ringer solution to test in vitro biodegradation behaviour show only small fluctuations in pH and conductivity.

Keywords
nonisocyanate polyurethanes, NIPU, POSS, porous materials, particle leaching

1. INTRODUCTION

Due to their outstanding properties, polyurethanes (PUs) are used extensively in industries such as construction, biomedicine, and automotive, where they function as thermosets or thermoplastics (Bizet et al., 2020). Conventionally, PUs are synthesized from polyols and diisocyanates (Guan et al., 2011). However, the high reactivity of diisocyanates poses serious health risks, including asthma, respiratory and skin irritation, and dermatitis (Bello et al., 2004; Liu et al., 2006; Mapp et al., 1988; Vijayan, 2010). Moreover, industrial isocyanate synthesis requires toxic phosgene (Figovsky et al., 2012; Kathalewar et al., 2013), which can cause severe lung damage upon exposure (Chen et al., 2017).

Non-isocyanate polyurethanes (NIPUs) offer a safer and more sustainable alternative. Numerous studies have shown that NIPUs can provide improved thermal, chemical, or even mechanical resistance compared to traditional PUs, without relying on hazardous reagents (Booysen et al., 2015; Caló et al., 2002; Camara et al., 2014; Diakoumakos and Kotzev, 2004; Levina et al., 2014; Lee et al., 2024; Ochiai et al., 2005). While their mechanical performance still often lags behind that of conventional PUs (Choong et al., 2023; Ozimek and Pielichowski, 2024), their environmental benefits are clear: they avoid isocyanates, enable CO_2 uptake during cyclic carbonate synthesis, and contribute to decarbonization strategies (He et al., 2019).

The key advantage of NIPUs lies in their compatibility with green and renewable feedstocks, which continues to expand, as reviewed in (Choong et al., 2023; He et al., 2019; Mo et al., 2024; Ozimek and Pielichowski, 2024). Notable examples include CO_2-based monomers, soybean oil-derived cyclic carbonates, and lignin- or tannin-based systems that provide fire resistance and strong adhesive properties for structural or wood-composite foams (Iswanto et al., 2023; Lee et al., 2024). Lignin can also serve as a precursor for NIPU-suitable polyamines (Li et al., 2024). In addition, bis-cyclic carbonate synthesis protocols are developing rapidly with new mild and effective catalysts recently reported (Choong et al., 2023). Furthermore, recent progress in bis-cyclic carbonate synthesis under mild catalytic conditions supports the development of recyclable, solvent-free polyurethanes aligned with circular economy principles (He et al., 2019).

The most common route for NIPU synthesis involves reacting cyclic carbonates with diamines, a process that inherently captures CO_2 (Ozimek and Pielichowski, 2024; Rokicki et al., 2015). Nanostructured additives like polyhedral oligomeric silsesquioxane (POSS) are increasingly explored in PU systems for their ability to enhance thermal stability, fire resistance, and mechanical strength while improving compatibility with bio-fillers and lowering water uptake (de Hoyos-Martinez et al., 2024; Hebda et al., 2015; Hebda et al., 2018; Kalia and Pielichowski, 2018; Pagacz et al., 2016; Pielichowski et al., 2006; Strakowska et al., 2020). In

NIPU matrices, POSS has demonstrated further potential, with recent hybrid systems showing improved UV resistance, stiffness, and thermal degradation profiles (Liu et al., 2015; Liu et al., 2016). In parallel, hybrid polymerization methods combining step-growth and chain-growth processes, are gaining traction as ways to optimize NIPU network structure and performance (Bukowczan et al., 2024; Lambeth, 2021).

Preparation of porous NIPU materials has gained recent attention, though well-documented studies remain limited. Several groups have successfully fabricated NIPU foams using external blowing agents such as CO_2 or H_2 (El Khezraji et al., 2023; Stachak et al., 2021). Cornille et al. (2015) employed poly(methylhydrogenosiloxane) as a blowing agent in a carbonate–amine aminolysis system, yielding materials suitable for furniture or automotive applications. Valette et al. (2023) synthesized partially biobased flexible foams via transurethane polycondensation using fatty biscarbamates, diols, and diamines, with water/ethanol used as blowing agents. Grignard et al. (2016) produced microcellular NIPU foams with low thermal conductivity (50 mW/m·K) using supercritical CO_2. Smith et al. (2022) developed tannic-acid-based NIPU foams with glutaraldehyde and carboxylic acids, which showed outstanding flame resistance and thermal stability, delaying degradation by over 100 °C compared to PU foams.

Another approach for fabricating porous NIPUs involves self-blowing reactions, in which gas is generated in situ by reactive components (El Khezraji et al., 2023; Stachak et al., 2021). Clark et al. (2018) demonstrated a solvent-free method using a sorbitol-based bis-carbonate and diamines like cadaverine and hexamethylenediamine, producing insulating foams such as CO_2 evolved during polymerization. Similarly, Anitha et al. (2022) used cyclic carbonates and amine-terminated oligomers to form foams via CO_2 release. In a related strategy, thiolactone–amine chemistry was applied to generate recyclable, self-blown NIPUs that emulate conventional foams while offering closed-loop sustainability (Monie et al., 2022). Another way is to use amine-CO_2 adducts that work both as a foam generator and as a monomer (Choong et al., 2023).

One of the most versatile techniques for creating porous polymeric materials is the porogen-leaching method, also known as solvent casting and particulate leaching (SCPL). This approach disperses solid particles, typically salts like sodium chloride, into a polymer solution. To achieve uniform pore formation, the solution must possess suitable viscosity to prevent sedimentation. After a polymer matrix is formed, the porogen is leached out using water or another solvent, producing a defined porous network. For hydrophilic polymers such as many NIPUs that contain abundant hydroxyl groups (Łukaszewska et al., 2023), water alone can act as a leaching medium, minimizing the use of organic solvents and limiting particle settling.

This method enables precise control over pore size, shape, and interconnectivity, properties that are particularly advantageous for biomedical applications like tissue scaffolds (Janik and Marzec, 2015; Murphy et al., 2002). Although well established for conventional polyurethanes and PU composites (Chia et al., 2019), porogen leaching remains underutilized in NIPU systems. However, the hydroxyl-rich and water-compatible nature of NIPUs makes them ideal candidates for this solvent-free porosity generation method. Given their favourable water absorption and adjustable porosity, NIPUs are increasingly being considered for drug delivery and tissue engineering (Aduba et al., 2018).

To the best of our knowledge, the particle leaching method has not yet been applied to NIPU-POSS hybrid systems, despite its established use in biomedical polymer fabrication (Chia et al., 2019). This approach involves incorporating salt particles (typically 5–20%) into a polymer solution, followed by solvent removal and subsequent leaching with water or another solvent to form a porous matrix (Janik and Marzec, 2015). By adjusting particle size and concentration, the porosity of the resulting material can be finely tuned Draghi et al., 2005; Murphy et al., 2002; Zhang et al., 2005). Although this technique is well described for conventional PU foams (Heijkants et al., 2006; Sin et al., 2010), its usage to obtain NIPU porous materials has not been mentioned yet.

Hence, this study reports the application of the particle leaching method to synthesize porous NIPU and NIPU/POSS hybrid materials. The impact of POSS incorporation on the pore generation process was investigated using SEM and μ-CT imaging. These porous systems, prepared from hydroxyl-rich NIPUs, offer high structural control, in vitro aqueous stability, and promising characteristics for green, biocompatible scaffolds.

2. EXPERIMENTAL

2.1. Materials

The five-membered cyclic, trimethylpropanol tricyclocarbonate (TMP Tricarbonate) was obtained from Specific Polymers (Castries, France). Jeffamine D-400 (PPO diamine) was purchased from Huntsman (The Woodlands, Texas, USA), and triglycidylisobutyl POSS (3epPOSS or POSS) was purchased from Hybrid Plastics (EP0423, Hattiesburg, Mississippi, USA). Under normal conditions of temperature and pressure, triglycidylisobutyl POSS is a semitransparent, viscous liquid. 1,4-diaminebutane (DAB), 1,5,7-triazabicyclo[4.4.0]dec-5-ene (TBD), N,N′-dimethylacetamide (DMAc), Tetrabutylammonium bromide (TBAB), Tetrabutylammonium iodide (TBAI) and sodium bicarbonate (SB) were obtained from SigmaAldrich (Darmstadt, Germany). Ringer-Fresenius solution with the following composition (g/1000 ml): sodium chloride (8.6); potassium chloride (0.3); calcium chloride dihydrate (0.33); water for injection up to 1000 ml was used.

2.2. Methods

The reaction was monitored by Fourier infrared spectroscopy (FTIR) using a Nicolet iS5 spectrometer (Thermo Fisher Scientific, Waltham, MA, USA), equipped with an ATR attachment. FTIR analysis was performed in the wavelength range of 4000–400 cm^{-1}, with a scanning resolution of 4 cm^{-1} and a data interval of 0.482 cm^{-1}.

The JSM-6010LA (JEOL Ltd., Akishima, Tokyo, Japan) scanning electron microscope (SEM) was used to obtain microphotographs of the foamed materials. The samples were coated with a 4 nm layer of gold. The microphotographs were taken at a working distance of 10 mm with a voltage of 20 kV.

X-ray computer micro-tomography (μ-CT) was performed using a Nanotom 180 N device (GE Sensing & Inspection Technologies, Pforzheim, Germany), equipped with a nanofocus X-ray tube with a maximum voltage of 180 kV and Hamamatsu 2300 x 2300-pixel detector. DatosX software with the use of the Feldkamp algorithm for cone beam X-ray CT was used. The samples were scanned at a source voltage of 60 kV and 310 µA current, with a rotation of the sample of 360 ° in 1,800 steps. The exposure time was 500 ms and the resulting scanning time was 90 min. Frame averaging of 5 and image skip of 1 were applied. The reconstructed images had a voxel size of 2.5 μm^3.

In submersion studies, the materials were placed in containers with a conical bottom and filled with Ringer solution. The containers were placed in an incubator at 36.6 °C for a total of 4 weeks. The pH and conductivity tests were carried out at 2–3 day intervals, using an ERH-111 pH electrode and a CD-2 conductivity probe, connected to a CPC-411 multimeter (HYDROMET SC, Tomaszów Mazowiecki, Poland).

2.3. Synthesis

The synthesis of the NIPU matrix and the NIPU/POSS composites was described in detail in (Raftopoulos et al., 2022). In summary, a two-step process was used. In the prepolymerization step, TMP tricarbonate and PPO diamine were reacted in DMAc as a solvent and in the presence of TBD as a catalyst. In the case of composites, Triglycidylisobutyl POSS was chemically incorporated into the NIPU matrix by the reaction of oxirane rings with amine groups – Scheme 1. POSS was added in a quantity of 5, 10, or 15 wt.% with respect to prepolymer mass, with TBAB and TBAI mixture (1:1 wt.) used as a catalyst system. In the chain extension step, DAB was added to the reaction mixture. The polymer mixture was poured into cylindrical glass vessels and then sodium bicarbonate with a particle diameter in the range of 0.05 to 0.315 mm was added at concentrations of 1:1 with

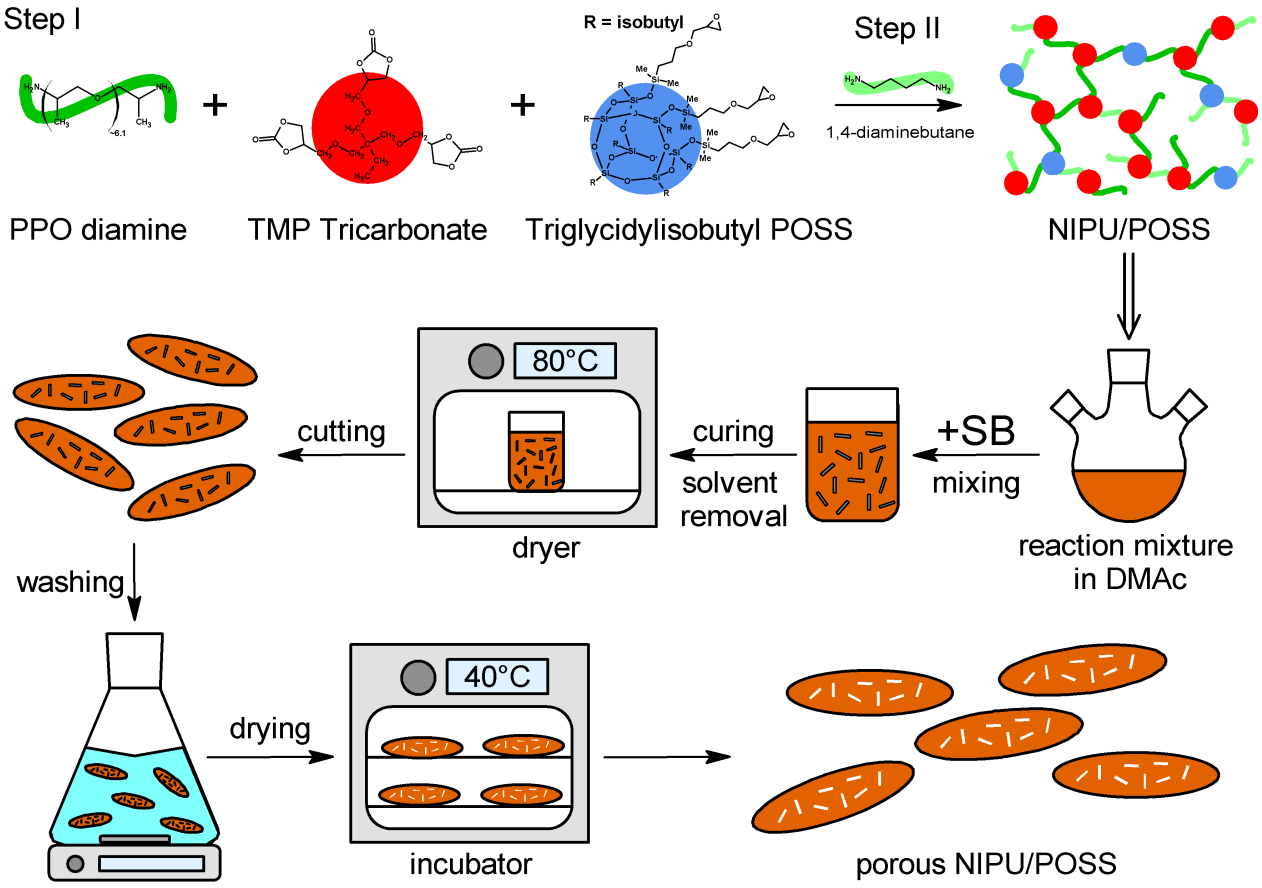

Scheme 1. Preparation of a porous NIPU/POSS system using the particle leaching method with SB.

respect to the total dry weight of the reagents. A portion of the respective reaction mixtures, without the addition of SB, was poured into separate containers for comparison. The NIPU/POSS system was cured and conditioned at 80 °C in a dryer for 3 days. In the next step, the samples were cut into slices and placed in flasks filled with water and placed on a magnetic stirrer to wash the salt for two weeks. After the washing period, the samples were placed in an incubator to dry at 40 °C for 1 week.

3. RESULTS AND DISCUSSION

FTIR spectra of the NIPU matrix, taken during various stages of the synthesis, are shown in Figure 1. The stretching vibrations of the carbonyl group in the cyclic carbonate are represented by the band at 1800 cm^{-1}, whereby the stretching of carbonyl moieties in urethane groups are evidenced by the band at 1720 cm^{-1} (Figure 1b). With the progress of the reaction, the intensity of the band corresponding to cyclic carbonates decreases, while the intensity of the band corresponding to urethanes increases. The broad band at 3250–3500 cm^{-1} (Figure 1a) corresponds to stretching vibrations of the –NH moiety in urethane group as well as those in the –OH groups, which are being formed during the opening of cyclic carbonate ring (Chen et al., 2017). The aforementioned changes in observed spectra are further pronounced after the chain extension step. Analogous observations are made for the FTIR spectra of the NIPU/POSS compound with 15 wt.% of POSS (Figure 2a and 2b). Bands of stretching vibrations in the oxirane ring are observed around 840 cm^{-1} (Figure 2c). The decrease of this band indicates the occurrence of a reaction between oxirane rings present in POSS and amine groups in PPO diamine and DAB. The FTIR spectra of the NIPU/POSS composites with 5 and 10 wt.% of POSS were analogous.

Figure 3 shows SEM images of the NIPU matrix, foamed with SB with various particle sizes. The elongated shapes of the pores correspond to the shapes of the SB particles. Some spherical pores are also visible; they probably originate from left-over gasses (air, vapourising solvent) trapped within the material or partial degradation of sodium bicarbonate, although the latter hypothesis is unlikely, as the temperatures during the synthesis and conditioning were relatively low. The pores measured during post-processing of the SEM images correspond to the sizes of the SB particles used. This confirms the possibility of obtaining pores of the desired shapes and sizes by using sodium bicarbonate crystals of the appropriate fraction size; such pore shape and size control is of crucial importance for, e.g., development of biomedical scaffolds.

SEM images of NIPU/POSS composites containing various POSS concentrations, foamed with 0.15–0.315 mm SB particles, are collected in Figure 4. NIPU composites reinforced with silsesquioxanes exhibit the same behaviour in terms of pore forming as a matrix. The measured pore sizes match the size of the particle fraction of SB used. When SB of selected fraction size is used in the process, the shape of the pores obtained is retained, regardless of the POSS load. EDS measurements showed no trace of sodium Kα peak at 1.041 keV (Newbury and Ritchie, 2016), which proves complete sodium bicarbonate leaching.

Microtomography was used to perform an additional evaluation of the microstructure of foamed structures and to assess the influence of POSS on their formation. Figure 5

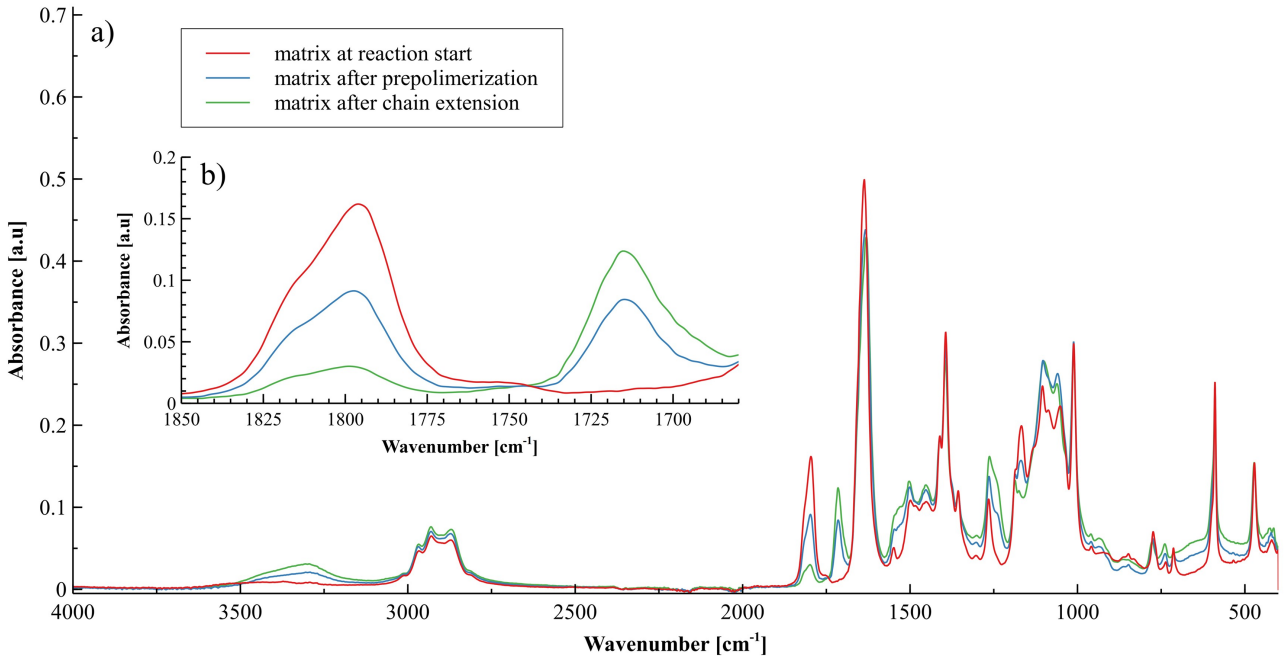

Figure 1. FTIR spectra at various stages of the synthesis of the NIPU matrix.

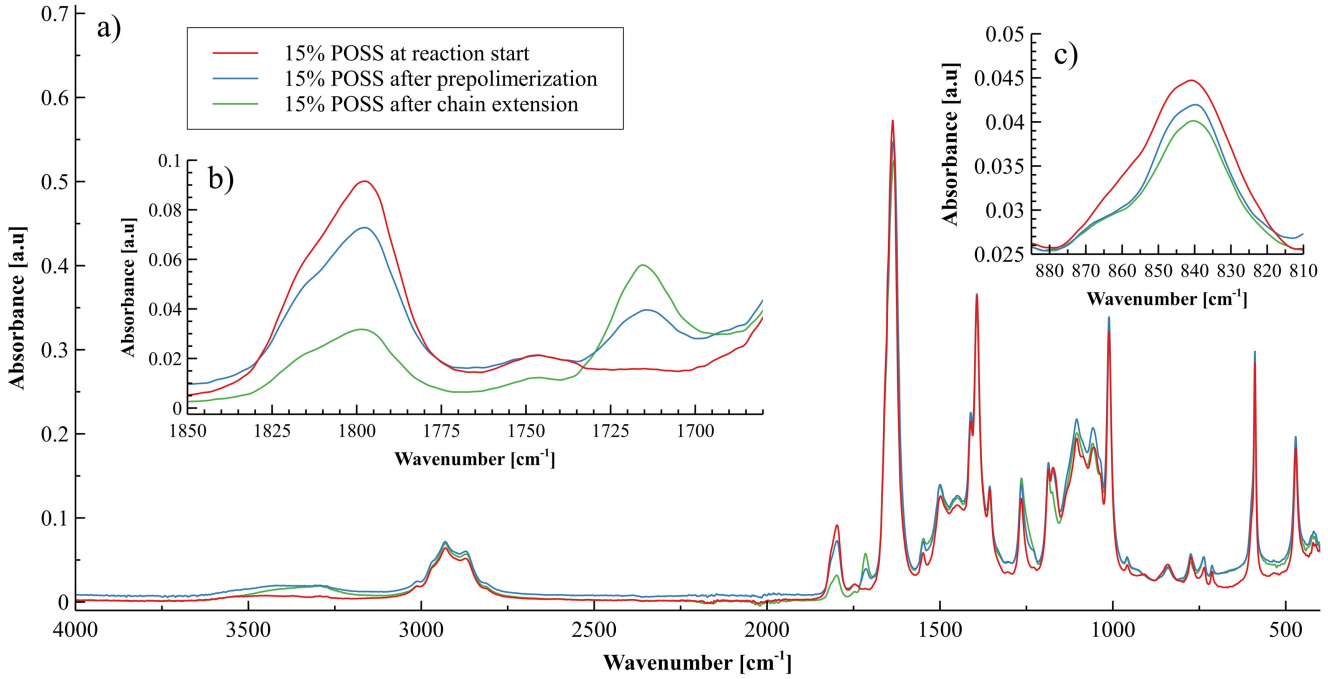

Figure 2. FTIR spectra at various stages of the synthesis of the 15 wt.% POSS composite.

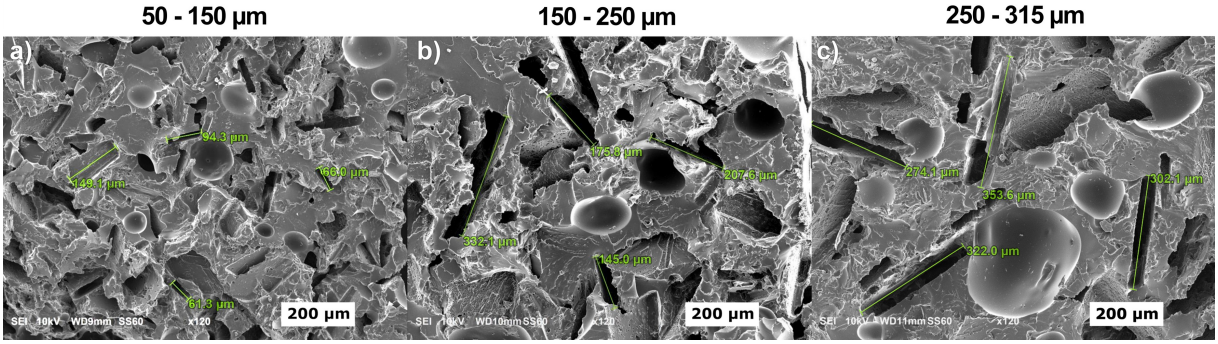

Figure 3. SEM images of NIPU matrix, foamed using the particle leaching method with various particle sizes of sodium bicarbonate. The applied spotsize (SS) was 60, and magnification x120.

shows μ-CT cross-sections, generated for the NIPU matrix and NIPU/POSS composites with various POSS content, foamed with SB particles of 0.15–0.315 mm.

The μ-CT confirms observations made previously during the analysis of SEM images. Proper selection of SB crystals with desired fraction size leads to the formation of uniformly shaped pores in NIPU matrices, the shape and size of which resemble the dimensions of SB crystals. The said dimensions are retained, regardless of the amount of POSS added. The pores have a flattened plate-shaped shape with dimensions ranging from 0.1 mm to 0.3 mm and 40–90 µm thick as presented in Figure 5. In addition to pores of this type, we also observe larger pores, which result from apparatus reasons – mainly due to air taken during mixing or evaporation of the solvent in the dryer. Degassing the samples in vacuum before crosslinking in the dryer could reduce their number. However, the high homogeneity and distribution of the pores created by the porogen-leaching method is clearly visible. The pore homogeneity is illustrated in the histogram in Figure 6. While the average pore size remains relatively consistent across samples, the material containing 5 wt.% POSS shows the broadest pore size distribution. It also exhibits the lowest total pore volume, likely due to initial network densification caused by low concentrations of trifunctional POSS. At higher POSS loadings, the pore volume remains relatively unchanged, possibly due to aggregation of POSS-containing segments, which limits further network compaction.

Since non-isocyanate polyurethanes, thanks to their non-toxicity and desirable properties, are considered as promising polymeric materials for biomedical applications (Aduba et al., 2018; Cornille et al., 2016; Ozimek and Pielichowski, 2022; Wendels and Avérous, 2021) we have performed initial in vitro tests using Ringer's solution to monitor the pH and conductivity changes, providing preliminary information on their biocompatibility.

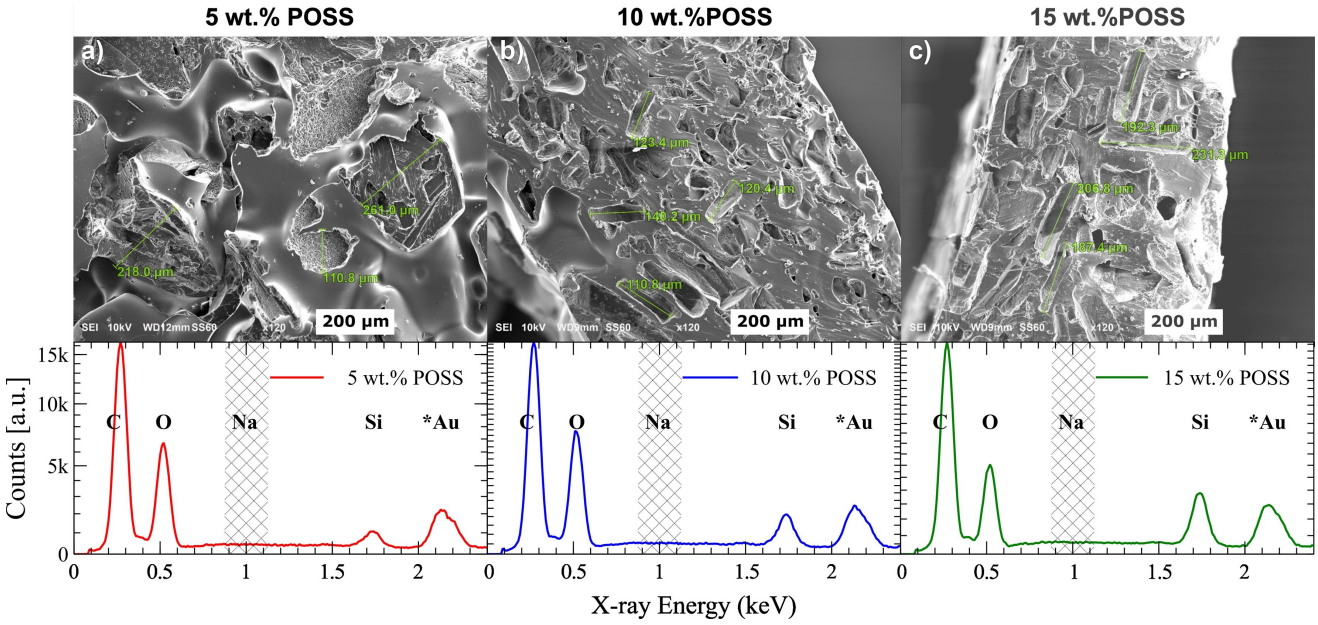

Figure 4. SEM images of NIPU/POSS compounds containing various amounts of POSS, foamed using the particle leaching method with 0.15–0.315 mm sodium bicarbonate particles. SS 60 and x120 magnification were used. Below the EDS measurements identifying the present elements. The grey checkered field marks the place where the sodium signal should appear.

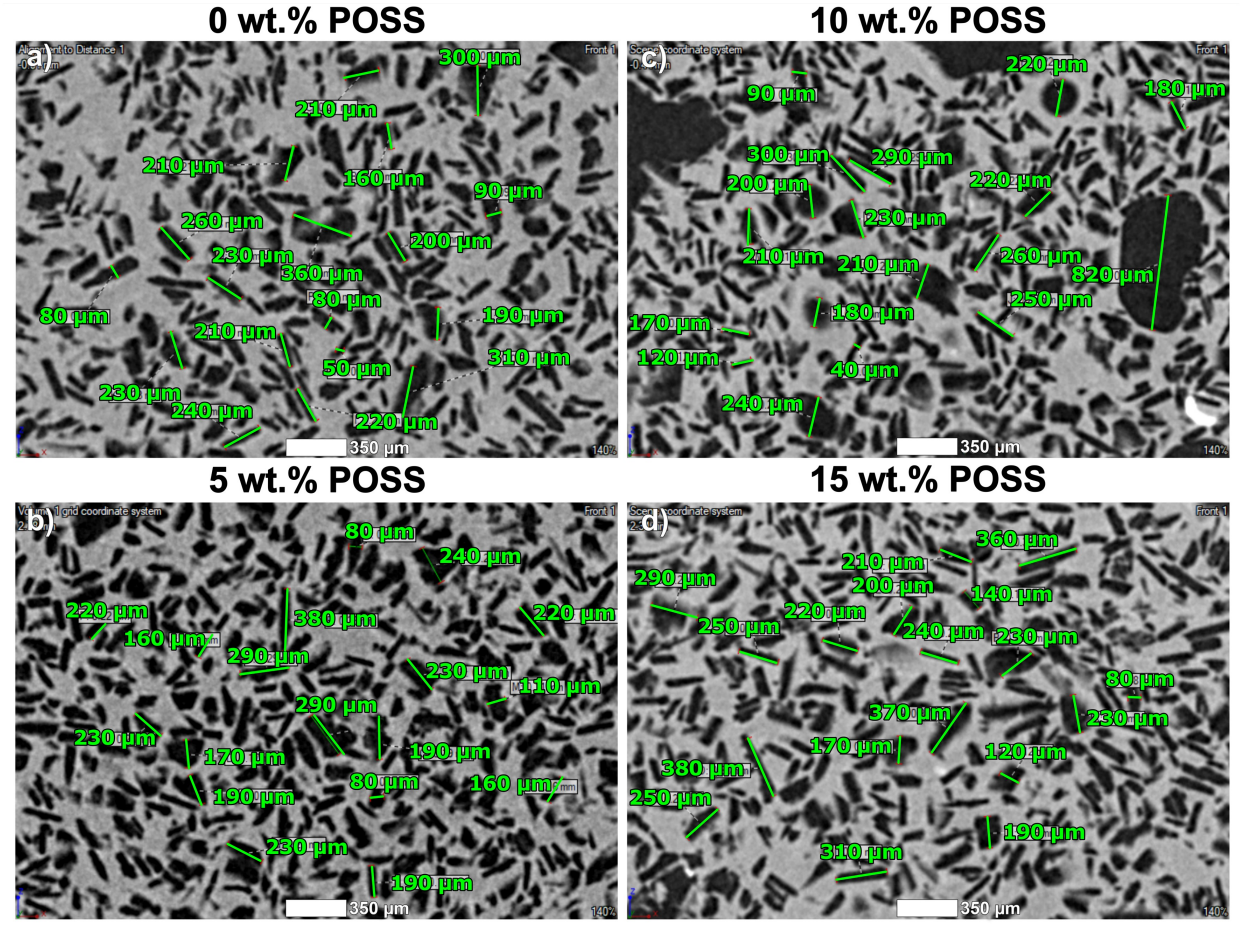

Figure 5. The μ-CT images of selected cross sections of NIPU matrix and NIPU/POSS compounds containing various amounts of POSS, foamed using the particle leaching method with SB particles of 0.15–0.315 mm.

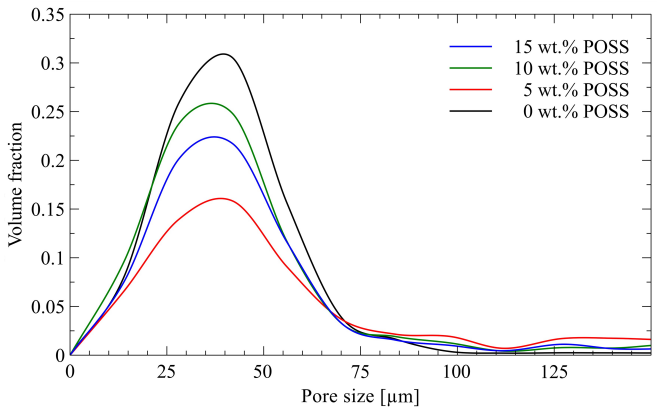

Figure 6. Pore size to volume fraction distribution for each material.

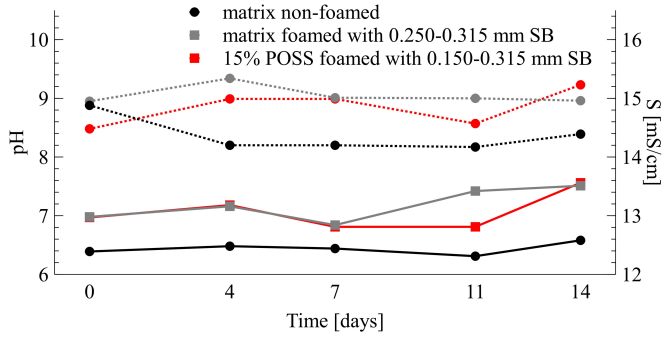

Figure 7. Fluctuations in pH (solid lines) and conductivity (S) (dotted lines) over time for Ringer's solution during submersion tests of selected matrix composite samples.

Table 1 shows pH and conductivity values of Ringer's solution with respective selected samples submerged in it. The pH and conductivity balance values for pure Ringer's solution are 6.67 and 14.1 mS/cm, respectively (Simionescu et al., 2020). Significant fluctuations, as well as deviations from both pH and conductivity values of those for the pure Ringer's solution, are undesirable. The values obtained for the non-foamed NIPU matrix bear the closest resemblance to those of the pure Ringer's solution.

Figure 7 shows pH and conductivity fluctuations over time for the Ringer's solution during the submersion test of selected NIPU and NIPU composites with POSS. Changes in pH and conductivity values during the studied period are not of high magnitude, which is a good premise for future biomedical applications of NIPU/POSS hybrid materials. However, more biological studies are planned to be performed in future research.

To evaluate the effect of 3epPOSS on the mechanical and thermal properties of the NIPU matrix, the Dynamic Mechanical Analysis (DMA) was used. Figure 8 presents the temperature-dependent storage modulus E′ (Figure 8a) and tan δ (Figure 8b) curves for the matrix and composite materials.

The matrix exhibits the highest glassy modulus (E′g = 2530 MPa) and α-relaxation temperature ($T\alpha$ = 36.3 °C), which reflects a well-structured, densely crosslinked network. Incorporation of POSS leads to softening and shift in transition temperature (15 wt.% POSS: E′g = 2169 MPa, and $T\alpha$ = 15.3 °C), indicating a loosening of the polymer network and crosslinking tightness. This behaviour may be attributed

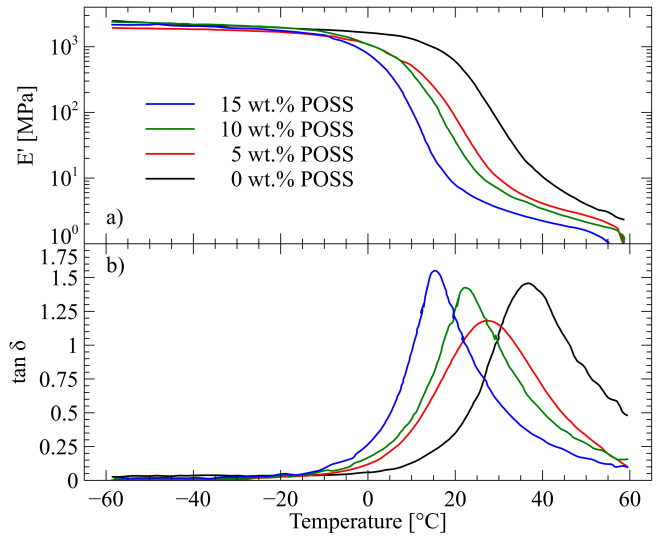

Figure 8. DMA curves for the matrix and composites 5, 10 and 15 wt.% POSS in the function of temperature: a) storage modulus E′, b) tan δ.

to the various effects i.e. disruption of polymer packaging, plasticization effect, and reduced entanglement and crosslinking density, especially when POSS is partially reacted with amine (Chen, 2016; Raftopoulos et al., 2022; Talik et al., 2018). Notably, the narrower and lower-temperature tan δ peaks for POSS-containing samples confirm increased chain mobility and reduced network integrity. These effects, while detrimental to stiffness, may enhance elasticity or degradability, which could be advantageous in specific biomedical applications.

Table 1. The pH and conductivity, S, values of the Ringer's solution for the studied samples.

Sample	pH			S [mS/cm]		
	Min	Max	Average	Min	Max	Average
Matrix non-foamed	6.31	6.58	6.44	14.17	14.88	14.37
Matrix foamed with 0.150–0.315 mm SB	6.84	7.51	7.18	14.95	15.34	15.05
15 wt.% POSS foamed with 0.150–0.315 mm SB	6.81	7.56	7.07	14.48	15.23	14.85

4. CONCLUSIONS

In this study, nonisocyanate polyurethane (NIPU) was synthesized in a reaction between trifunctional cyclic carbonate with poly (propylene oxide) derived diamine and 1,4-diaminebutane in a two-step process. The obtained NIPU formulation was chemically modified with polyhedral oligomeric silsesquioxane (POSS) moieties to obtain NIPU/POSS hybrids. The particle leaching method, involving the use of sodium bicarbonate, proved to be an effective technique to obtain foamed NIPU and foamed NIPU/POSS materials. The FTIR study confirmed the reaction between cyclic carbonates and amines, as well as the successful modification of the NIPU matrix with POSS particles via the reaction of amines and oxirane rings present in POSS. The SEM images confirmed that the materials obtained contained embedded pores, with a size corresponding to the size of the sodium bicarbonate fraction used to generate them. The addition of POSS moieties did not affect the shape nor the size of the obtained pores, as evidenced by analysis of SEM images. Pore diameters ranged between 110 μm to 260 μm. The same can be concluded on μ-CT scans. Quantitative μ-CT analysis revealed a reduction in total pore volume from 0.305 % for unmodified NIPU, to 0.158 % at 5 wt.% POSS, followed by stabilization at higher POSS loadings. This proves that, by utilising the particle leaching method, it is possible to obtain NIPU/POSS hybrid porous materials with tailored pore architectures, crucial for material design across multiple sectors. In vitro tests using Ringer's solution revealed that the pH and conductivity values over the studied period did not differ significantly. Specifically, pH values remained within 6.4 and 7.6, while conductivity stabilized at 14.2 to 15.4 mS/cm during the whole 14 days. That is of crucial importance for future biomedical applications of NIPU/POSS hybrid materials, which may be (but are not limited to) tissue scaffolds or drug-delivery hydrogel materials. Moreover, DMA measurements revealed that increasing POSS content led to lowering glassy modulus for the matrix from 2530 MPa to 2169 MPa for 15 wt.% POSS and α-relaxation temperatures from 36.3 °C to 15.3 °C respectively, indicating reduced network stiffness and enhanced chain mobility due to POSS-induced disruption of polymer packing, which enhance elasticity, and may ease their degradability. In other fields, their potential can further extend to smart packaging, insulation foams in low-carbon construction, or even advanced nanocomposites for energy storage applications – especially when POSS is used to enhance dielectric or thermal performance.

This work demonstrates the first successful application of the particle leaching method to fabricate porous NIPU/POSS materials with controlled pore morphology, biocompatible aqueous response, and tunable mechanical properties. The porous NIPU/POSS hybrid system described herein represents only a fraction of NIPU materials and composites, incorporating environmentally friendly reagents. However, it shows a broad potential to replace conventional polyurethanes in eco-conscious applications across biomedical, construction, and energy fields.

ACKNOWLEDGEMENTS

The authors are grateful to the Polish National Science Centre for support under Contract No. 2017/27/B/ST8/01584.

REFERENCES

Aduba D.C., Zhang K., Kanitkar A., Sirrine J.M., Verbridge S.S., Long T.E., 2018. Electrospinning of plant oil-based, non-isocyanate polyurethanes for biomedical applications. *J. Appl. Polym. Sci.*, 135, 46464. DOI: 10.1002/app.46464.

Anitha S., Unnikrishnan G., Santhosh Kumar K.S., 2022. Self-blowing non-isocyanate polyurethane foam: synthesis, characterization and properties. *Mater. Lett.: X*, 14, 100142. DOI: 10.1016/j.mlblux.2022.100142.

Bello D., Woskie S.R., Streicher R.P., Liu Y., Stowe M.H., Eisen E.A., Ellenbecker M.J., Sparer J., Youngs F., Cullen M.R., Redlich C.A., 2004. Polyisocyanates in occupational environments: A critical review of exposure limits and metrics. *Am. J. Ind. Med.*, 46, 480–491. DOI: 10.1002/ajim.20076.

Bizet B., Grau É., Cramail H., Asua J.M., 2020. Water-based non-isocyanate polyurethane ureas (NIPUUs). *Polym. Chem.*, 11, 3786–3799. DOI: 10.1039/D0PY00427H.

Booysen J., Marx S., Muller L., Vermeulen U., Grobler A., 2015. Synthesis of novel non-isocyanate polyhydroxyurethane from L-Lysine and its application. *7th Int. Conf. Latest Trends Eng. Technol.*, Pretoria, South Africa, 2–5 July 2015.

Bukowczan A., Łukaszewska I., Pielichowski K., 2024. Thermal degradation of non-isocyanate polyurethanes. *J. Therm. Anal. Calorim.*, 149, 10885–10899. DOI: 10.1007/s10973-024-13306-1.

Caló V., Nacci A., Monopoli A., Fanizzi A., 2002. Cyclic carbonate formation from carbon dioxide and oxiranes in tetrabutylammonium halides as solvents and catalysts. *Org. Lett.*, 4, 2561–2563. DOI: 10.1021/ol026189w.

Camara F., Benyahya S., Besse V., Boutevin G., Auvergne R., Boutevin B., Caillol S., 2014. Reactivity of secondary amines for the synthesis of non-isocyanate polyurethanes. *Eur. Polym. J.*, 55, 17–26. DOI: 10.1016/j.eurpolymj.2014.03.011.

Chen J.Z.Y., 2016. Theory of wormlike polymer chains in confinement. *Prog. Polym. Sci.*, 54–55, 3–46. DOI: 10.1016/j.progpolymsci.2015.09.002.

Chen L., Wu D., Kim J.-M., Yoon J., 2017. An ESIPT-based fluorescence probe for colorimetric, ratiometric, and selective detection of phosgene. *Anal. Chem.*, 89, 12596–12601. DOI: 10.1021/acs.analchem.7b03988.

Chia O.C., Suhaimin I.S., Kassim S.A., Zubir S.A., Abdullah T.K., 2019. Effect of modified solvent casting/particulate leaching (SCPL) technique on the properties of bioactive glass reinforced polyurethane scaffold for biomedical applications. *J. Phys. Sci.*, 30(Suppl. 2), 115–126. DOI: 10.21315/jps2019.30.s2.10.

Choong P.S., Hui Y.L.E., Lim C.C., 2023. CO_2-blown nonisocyanate polyurethane foams. *ACS Macro Lett.*, 12, 1094–1099. DOI: 10.1021/acsmacrolett.3c00334.

Clark J.H., Farmer T.J., Ingram I.D.V., Lie Y., North M., 2018. Renewable self-blowing non-isocyanate polyurethane foams from lysine and sorbitol. *Eur. J. Org. Chem.*, 31, 4265–4271. DOI: 10.1002/ejoc.201800665.

Cornille A., Dworakowska S., Bogdal D., Boutevin B., Caillol S., 2015. A new way of creating cellular polyurethane materials: NIPU foams. *Eur. Polym. J.*, 66, 129–138. DOI: 10.1016/j.eurpolymj.2015.01.034.

Cornille A., Guillet C., Benyahya S., Negrell C., Boutevin B., Caillol S., 2016. Room temperature flexible isocyanate-free polyurethane foams. *Eur. Polym. J.*, 84, 873–888. DOI: 10.1016/j.eurpolymj.2016.05.032.

de Hoyos-Martinez P.L., Mendez S.B., Martinez E.C., Wang D.Y., Labidi J., 2024. Elaboration of thermally performing polyurethane foams based on biopolyols with thermal insulating applications. *Polymers*, 16, 258. DOI: 10.3390/polym16020258.

Diakoumakos C.D., Kotzev D.L., 2004. Non-isocyanate-based polyurethanes derived upon the reaction of amines with cyclocarbonate resins. *Macromol. Symp.*, 216, 37–46. DOI: 10.1002/masy.200451205.

Draghi L., Resta S., Pirozzolo M.G., Tanzi M.C., 2005. Microspheres leaching for scaffold porosity control. *J. Mater. Sci.: Mater. Med.*, 16, 1093–1097. DOI: 10.1007/s10856-005-4711-x.

El Khezraji S., Ben youcef H., Belachemi L., Lopez Manchado M.A., Verdejo R., Lahcini M., 2023. Recent progress of non-isocyanate polyurethane foam and their challenges. *Polymers*, 15, 254. DOI: 10.3390/polym15020254.

Figovsky O., Shapovalov L., Leykin A., Birukova O., Potashnikova R., 2012. Progress in elaboration of nonisocyanate polyurethanes based on cyclic carbonates. *Int. Lett. Chem. Phys. Astron.*, 3, 52–66. DOI: 10.56431/p-422370.

Grignard B., Thomassin J.-M., Gennen S., Poussard L., Bonnaud L., Raquez J.-M., Dubois P., Tran M.P., Park C.B., Jerome C., Detrembleur C., 2016. CO_2-blown microcellular non-isocyanate polyurethane (NIPU) foams: From bio- and CO_2-sourced monomers to potentially thermal insulating materials. *Green Chem.*, 18, 2206–2215. DOI: 10.1039/C5GC02723C.

Guan J., Song Y., Lin Y., Yin X., Zuo M., Zhao Y., Tao X., Zheng Q., 2011. Progress in study of non-isocyanate polyurethane. *Ind. Eng. Chem. Res.*, 50, 6517–6527. DOI: 10.1021/ie101995j.

He X., Xu X., Wan Q., Bo G., Yan Y., 2019. Solvent- and catalyst-free synthesis, hybridization and characterization of biobased nonisocyanate polyurethane (NIPU). *Polymers*, 11, 1026. DOI: 10.3390/polym11061026.

Hebda E., Bukowczan A., Ozimek J., Raftopoulos K.N., Wroński S., Tarasiuk J., Pielichowski J., Leszczyńska A., Pielichowski K., 2018. Rigid polyurethane foams reinforced with disilanolisobutyl POSS: Synthesis and properties. *Polym. Adv. Technol.*, 29, 1879–1888. DOI: 10.1002/pat.4296.

Hebda E., Ozimek J., Raftopoulos K.N., Michałowski S., Pielichowski J., Jancia M., Pielichowski K., 2015. Synthesis and morphology of rigid polyurethane foams with POSS as pendant groups or chemical crosslinks. *Polym. Adv. Technol.*, 26, 932–940. DOI: 10.1002/pat.3504.

Heijkants R.G.J.C., Van Tienen T.G., De Groot J.H., Pennings A.J., Buma P., Veth R.P.H., Schouten A.J., 2006. Preparation of a polyurethane scaffold for tissue engineering made by a combination of salt leaching and freeze-drying of dioxane. *J. Mater. Sci.*, 41, 2423–2428. DOI: 10.1007/s10853-006-7065-y.

Iswanto A.H., Lubis M.A.R., Sutiawan J., Al-Edrus S.S.O., Lee S.H., Antov P., Kristak L., Reh R., Mardawati E., Santoso A., Kusumah S.S., 2023. Latest advancements in the development of high-performance lignin- and tannin-based non-isocyanate polyurethane adhesive for wood composites. *Polymers*, 15, 3864. DOI: 10.3390/polym15193864.

Janik H., Marzec M., 2015. A review: Fabrication of porous polyurethane scaffolds. *Mater. Sci. Eng. C*, 48, 586–591. DOI: 10.1016/j.msec.2014.12.037.

Kalia S., Pielichowski K., 2018. *Polymer/POSS nanocomposites and hybrid materials*. Springer, Cham. DOI: 10.1007/978-3-030-02327-0.

Kathalewar M.S., Joshi P.B., Sabnis A.S., Malshe V.C., 2013. Non-isocyanate polyurethanes: From chemistry to applications. *RSC Adv.*, 3, 4110–4129. DOI: 10.1039/c2ra21938g.

Lambeth R.H., 2021. Progress in hybrid non-isocyanate polyurethanes. *Polym. Int.*, 70, 696–700. DOI: 10.1002/pi.6078.

Lee G.R., Lee E.J., Shin H.S., Kim J., Kim I., Hong S.C., 2024. Preparation of non-isocyanate polyurethanes from mixed cyclic-carbonated compounds: Soybean oil and CO_2-based poly(ether carbonate). *Polymers*, 16, 1171. DOI: 10.3390/polym16081171.

Levina M.A., Krasheninnikov V.G., Zabalov M.V., Tiger R.P., 2014. Nonisocyanate polyurethanes from amines and cyclic carbonates: Kinetics and mechanism of a model reaction. *Polym. Sci. Ser. B*, 56, 139–147. DOI: 10.1134/S1560090414020092.

Li Y., Li J., Ren B., Cheng H., 2024. Conversion of lignin to nitrogenous chemicals and functional materials. *Materials*, 17, 5110. DOI: 10.3390/ma17205110.

Liu G., Wu G., Chen J., Huo S., Jin C., Kong Z., 2015. Synthesis and properties of POSS-containing gallic acid-based non-isocyanate polyurethanes coatings. *Polym. Degrad. Stab.*, 121, 247–252. DOI: 10.1016/j.polymdegradstab.2015.09.013.

Liu G., Wu G., Chen J., Kong Z., 2016. Synthesis, modification and properties of rosin-based non-isocyanate polyurethanes coatings. *Prog. Org. Coat.*, 101, 461–467. DOI: 10.1016/j.porgcoat.2016.09.019.

Liu Y., Stowe M.H., Bello D., Woskie S.R., Sparer J., Gore R., Youngs F., Cullen M.R., Redlich C.A., 2006. Respiratory protection from isocyanate exposure in the autobody repair and refinishing industry. *J. Occup. Environ. Hyg.*, 3, 234–249. DOI: 10.1080/15459620600628704.

Łukaszewska I., Bukowczan A., Raftopoulos K.N., Pielichowski K., 2023. 'Spider-like' POSS in NIPU webs: enhanced thermal stability and unique swelling behavior. *J. Polym. Res.*, 30, 456. DOI: 10.1007/s10965-023-03834-z.

Mapp C.E., Corona P.C., De Marzo N., Fabbri L., 1988. Persistent asthma due isocyanates. A follow-up study of subjects with occupational asthma due to toluene diisocyanate (TDI). *Am. Rev. Respir. Dis.*, 137, 1326–1329. DOI: 10.1164/ajrccm/137.6.1326.

Mo Y., Huang X., Hu C., 2024. Recent advances in the preparation and application of bio-based polyurethanes. *Polymers*, 16, 2155. DOI: 10.3390/polym16152155.

Monie F., Grignard B., Detrembleur C., 2022. Divergent aminolysis approach for constructing recyclable self-blown nonisocyanate polyurethane foams. *ACS Macro Lett.*, 11, 236–242. DOI: 10.1021/acsmacrolett.1c00793.

Murphy W.L., Dennis R.G., Kileny J.L., Mooney D.J., 2002. Salt fusion: an approach to improve pore interconnectivity within tissue engineering scaffolds. *Tissue Eng.*, 8, 43–52. DOI: 10.1089/107632702753503045.

Newbury D.E., Ritchie N.W.M., 2016. Measurement of trace constituents by electron-excited X-ray microanalysis with energy-dispersive spectrometry. *Microsc. Microanal.*, 22, 520–535. DOI: 10.1017/S1431927616000738.

Ochiai B., Satoh Y., Endo T., 2005. Nucleophilic polyaddition in water based on chemoselective reaction of cyclic carbonate with amine. *Green Chem.*, 7, 765–767. DOI: 10.1039/b511019j.

Ozimek J., Pielichowski K., 2022. Recent advances in polyurethane/POSS hybrids for biomedical applications. *Molecules*, 27, 40. DOI: 10.3390/molecules27010040.

Ozimek J., Pielichowski K., 2024. Sustainability of noniso-cyanate polyurethanes (NIPUs). *Sustainability*, 16, 9911. DOI: 10.3390/su16229911.

Pagacz J., Hebda E., Michałowski S., Ozimek J., Sternik D., Pielichowski K., 2016. Polyurethane foams chemically reinforced with POSS – thermal degradation studies. *Thermochim. Acta*, 642, 95–104. DOI: 10.1016/j.tca.2016.09.006.

Pielichowski K., Njuguna J., Janowski B., Pielichowski J., 2006. Polyhedral oligomeric silsesquioxanes (POSS)-containing nanohybrid polymers. In: AbeA., Dušek K., Kobayashi S. (Eds.), *Supramolecular polymers polymeric betains oligomers. advances in polymer science*. Springer, Berlin, Heidelberg. 201, 225–296. DOI: 10.1007/12_077.

Raftopoulos K.N., Łukaszewska I., Bujalance Calduch C., Stachak P., Lalik S., Hebda E., Marzec M., Pielichowski K., 2022. Hydration and glass transition of hybrid non-isocyanate polyurethanes with POSS inclusions. *Polymer*, 253, 125010. DOI: 10.1016/j.polymer.2022.125010.

Rokicki G., Parzuchowski P.G., Mazurek M., 2015. Non-isocyanate polyurethanes: Synthesis, properties, and applications. *Polym. Adv. Technol.*, 26, 707–761. DOI: 10.1002/pat.3522.

Simionescu N., Benea L., Chiriac A., 2020. The effect of H_2O2 and lactic acid addition in biological saliva on the corrosion behaviour of 304L stainless steel. *IOP Conf. Ser. Mater. Sci. Eng.*, 877, 012039. DOI: 10.1088/1757-899X/877/1/012039.

Sin D.C., Miao X., Liu G., Wei F., Chadwick G., Yan C., Friis T., 2010. Polyurethane (PU) scaffolds prepared by solvent casting/particulate leaching (SCPL) combined with centrifugation. *Mater. Sci. Eng. C*, 30, 78–85. DOI: 10.1016/j.msec.2009.09.002.

Smith D.L., Rodriguez-Melendez D., Cotton S.M., Quan Y., Wang Q., Grunlan J.C., 2022. Non-isocyanate polyurethane bio-foam with inherent heat and fire resistance. *Polymers*, 14, 5019. DOI: 10.3390/polym14225019.

Stachak P., Łukaszewska I., Hebda E., Pielichowski K., 2021. Recent advances in fabrication of non-isocyanate polyurethane-based composite materials. *Materials*, 14, 3497. DOI: 10.3390/ma14133497.

Strakowska A., Członka S., Kairytė A., 2020. Rigid polyurethane foams reinforced with POSS-impregnated sugar beet pulp filler. *Materials*, 13, 5493. DOI: 10.3390/ma13235493.

Talik A., Tarnacka M., Grudzka-Flak I., Maksym P., Geppert-Rybczynska M., Wolnica K., Kaminska E., Kaminski K., Paluch M., 2018. The role of interfacial energy and specific interactions on the behavior of poly(propylene glycol) derivatives under 2D confinement. *Macromolecules*, 51, 4840–4852. DOI: 10.1021/acs.macromol.8b00658.

Valette V., Kébir N., Burel F., Lecamp L., 2023. Design of biobased non-isocyanate polyurethane (NIPU) foams blown with water and/or ethanol. *Express Polym. Lett.*, 17, 974–990. DOI: 10.3144/expresspolymlett.2023.72.

Vijayan V.K., 2010. Methyl isocyanate (MIC) exposure and its consequences on human health at Bhopal. *Int. J. Environ. Stud.*, 67, 637–653. DOI: 10.1080/00207233.2010.515435.

Wendels S., Avérous L., 2021. Biobased polyurethanes for biomedical applications. *Bioact. Mater.*, 6, 1083–1106. DOI: 10.1016/j.bioactmat.2020.10.002.

Zhang J., Wu L., Jing D., Ding J., 2005. A comparative study of porous scaffolds with cubic and spherical macropores. *Polymer*, 46, 4979-4985. DOI: 10.1016/j.polymer.2005.02.120.